Journal of Applied Polymer Science

Synthesis and ferroelectric investigations of poly(vinylidene fluoride-*co*-hexafluoropropylene)-$Mg(NO_3)_2$ films

S. Divya, T. Shakthi, J. Hemalatha
Advanced Materials Lab, Department of Physics, National Institute of Technology, Tiruchirappalli, 620 015, India
Correspondence to: J. Hemalatha (E-mail: hemalatha@nitt.edu)

ABSTRACT: The free-standing, flexible, and ferroelectric films of poly(vinylidenefluoride-*co*-hexafluoropropylene) [P(VDF-HFP)] were prepared by spin coating method. The ferroelectric phase of the films was enhanced by adding magnesium nitrate $Mg(NO_3)_2$ in different wt % as the additive during the film fabrication. The effects on the structural, compositional, morphological, ferroelectric, dielectric, and leakage current behaviors of the films due to the addition of salt were analyzed. Based on the X-ray diffraction (XRD) patterns and Fourier Transform Infrared (FTIR) spectra, it is confirmed that the addition of $Mg(NO_3)_2$ promotes the electroactive β phase that induces the ferroelectric property. The fiber-like topography of the films exhibits a nodule-like structure, and the roughness of the films increases by the addition of $Mg(NO_3)_2$. The ferroelectric studies show the higher polarization values for the composite films than that of the plain P(VDF-HFP) film. The Piezo-response force microscope images also confirm the domain switching behavior of the samples. © 2016 Wiley Periodicals, Inc. J. Appl. Polym. Sci. **2016**, *133*, 44008.

KEYWORDS: copolymers; dielectric properties; films; microscopy; properties and characterization

Received 17 February 2016; accepted 1 June 2016
DOI: 10.1002/app.44008

INTRODUCTION

Recent advancements in micro/nano electromechanical devices require electroactive flexible films, which should combine significant ferroelectricity, favorable mechanical properties, and easy processibility. As a natural material that combines all the above is rare, it has become the focus of recent research[1–4] to induce ferroelectricity in the polymers which possess the other two properties. Among the variety of polymers, poly(vinylidenefluoride) (PVDF) and its co-polymers such as poly(vinylidenefluoride-*co*-hexafluoropropylene) [P(VDF-HFP)], poly(vinylidenefluoride-trifluoroethylene) [P(VDF-TrFE)], and poly(vinylidenefluoride-chlorotrifluoroethylene) [P(VDF-CTFE)] are well known for their ferroelectricity and piezoelectricity, since they have electro active polymorphic phases due to their more ordered structure that gives rise to a high dipole moment and dielectric constant.[5,6] They exhibit five crystalline phases α, β, γ, δ, and ε with different conformations,[7] which can transform to each other under specific conditions such as mechanical deformation, high temperature, and electric field.

P(VDF-HFP), a random co-polymer of PVDF, has interesting properties such as a high dielectric constant (8.4), low crystallinity, and low glass transition temperature (−35 °C) and hence, it is the ideal candidate for several applications, including electroacoustic and electromechanical convertors, actuators, ferroelectric memory devices, mechatronics, and artificial muscles.[8]

Constant efforts have been made by researchers to enhance the ferroelectric phases in the polymer film to get improved performance by poling, stretching, and by adding additives, nano fillers, etc. A brief review of such attempts is presented below.

He *et al.*[9] have reported an enhancement of the ferroelectric β phase when P(VDF-HFP)-$Mg(NO_3)_2$ is coated on a Si substrate and the remanent polarization is found to be 5.98 μC/cm^2 at 350 MV/m. Jayasuriya *et al.*[10] have studied the ferroelectric behaviors of P(VDF-HFP) films obtained through different preparation techniques. The remanent polarization values are reported to be 80 and 50 mC/m^2, respectively, for 5 and 15% hexafluoropropylene (HFP) molar content samples prepared by the solvent cast technique. However, the films prepared through the slow cooled technique are reported to exhibit no ferroelectric property. The stretched films of P(VDF-HFP) copolymer added with the kaolinite nano fillers are found to have a reduction in the remanent polarization, as per the report of Tomer *et al.*[11] Wegener *et al.*[12] observed, that the poled Lead Zirconate Titanate (PZT)/P(VDF-HFP) composite films have the coercive field and polarization values of 1.5 MV/m and 4.5 μC/cm^2, respectively, and also reported the maximum piezoelectric coefficient of 11×10^{-6} μCN^{-1} value.

The present work encompasses the fabrication of free-standing, flexible ferroelectric films of P(VDF-HFP), and a systematic

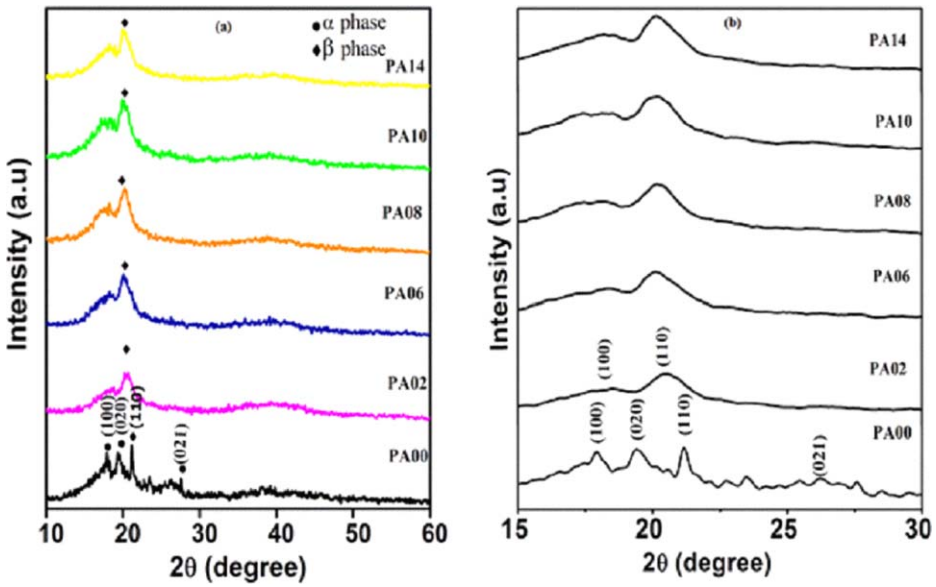

Figure 1. XRD patterns of P(VDF-HFP) film and P(VDF-HFP)-$Mg(NO_3)_2$ films for (a) 10–80 range and (b) 15–30 range of 2θ. [Color figure can be viewed in the online issue, which is available at wileyonlinelibrary.com.]

study of the enhancement of the electroactive phase in the films, through the incorporation of a $Mg(NO_3)_2$ additive.

EXPERIMENTAL

The chemicals used for the fabrication of the films were P(VDF-HFP) of molecular weight 130,000 purchased from Sigma Aldrich Co., USA, dimethylformamide [$(CH_3)_2NCH$], and magnesium nitrate [$Mg(NO_3)_2$] from Merck Specialities Private limited, Mumbai. The polymer solution obtained by dissolving P(VDF-HFP) in dimethylformamide (DMF) was used as the precursor and the films were fabricated using the spin coating method. Films of various thickness values were prepared at various drying temperatures. The films of thickness 120 μm, which are dried at 100 °C, were found to be free-standing and flexible whereas, the other films roll at the corners and they were not free-standing. So, the films of thickness 120 μm were prepared by optimizing the concentration of the polymer-DMF solution to be 0.2 wt %, drying temperature to be 100 °C, and by setting the spin at 250 rpm, and the rotation time of 5 sec in the spin coating unit. The P(VDF-HFP) films thus obtained were coded as PA00. To prepare the composite films, an appropriate amount of $Mg(NO_3)_2$ was dispersed uniformly in the polymer solution through vigorous stirring for 30 min, and then casted as films maintaining the above mentioned optimized conditions. The films loaded with 0.2, 0.6, 0.8, 1.0, and 1.4 wt % of magnesium nitrate were coded as PA02, PA06, PA08, PA10, and PA14, respectively.

The structural analyses of the films were made using an X-ray diffractometer pattern, obtained with Cu Kα1 radiation (λ = 0.15406 nm) for 2θ values ranging from 10 to 80° (Rigaku ultima 3). The Fourier Transform Infrared (FTIR) spectra of the samples were recorded on a Perkin Elmer spectrophotometer (Spectrum RX1), and the spectra were collected from 600 to 1,400 cm^{-1}. The morphological studies were done by taking Scanning Electron Microscope (SEM) images, using TEScan Vega-3 LMU. The surface roughness and topography studies were analyzed by Atomic Force Microscope (AFM) (Park system NX10) in the contact mode with a Si tip. The ferroelectric property and domain switching process were investigated by PiezoForce Microscopy (PFM). The ferroelectric hysteresis of polarization versus electric field was plotted at room temperature, using a sawyer tower circuit based PE loop tracer, by applying the maximum electric field of 30 MV/m, and using a

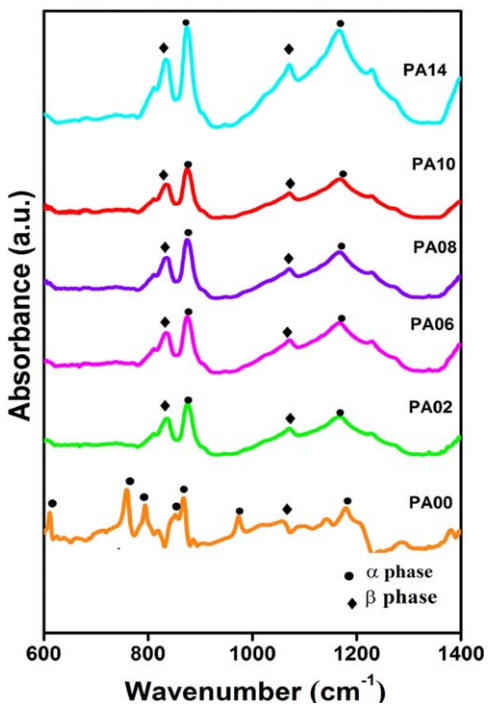

Figure 2. FTIR spectra of P(VDF-HFP) film and P(VDF-HFP)-$Mg(NO_3)_2$ films. [Color figure can be viewed in the online issue, which is available at wileyonlinelibrary.com.]

Table I. Characteristic Bands with Specific Vibrational Modes and Crystalline Phases

Sample code	Band (cm^{-1})	Phase	Vibration
PA00	612	α	—C—F— wagging modes (Ref. 16)
	757	α	CF_2 bending and skeletal bending (Ref. 18)
	794	α	CH_2 rocking of α (Ref. 18)
	855	α	CH out-of-plane deformation (Ref. 16)
	875	α	CC asymmetric stretching vibration (Ref. 16)
	977	α	CH out-of-plane deformation (Ref. 16)
	1070	β	Symmetric C—F stretching (Refs. 16-18)
	1179	α	Symmetrical stretching mode of CF_2 (Ref. 16)
PA02-PA14	836	β	CH_2 rocking of β (Ref. 18)
	875	α	CC asymmetric stretching vibration (Ref. 16)
	1070	β	Symmetric C—F stretching (Ref. 16)
	1165	α	CH_2 symmetric stretching mode (Ref. 18)
	1227	β	CF out-of-plane deformation (Ref. 17)

silver electrode of area 9 mm^2. The dielectric properties of all the films were studied at room temperature over the range of frequencies from 50 Hz to 100 kHz with the applied signal of 1 V, using an impedance analyzer (solartron). The leakage current measurements were made using an electrometer (6517A) from Keithley instruments over a range of voltage −30 to +30 V with a step voltage of 1 V and time delay of 7 sec.

RESULTS AND DISCUSSION

The X-ray diffraction (XRD) patterns of the plain P(VDF-HFP) film (PA00) and P(VDF-HFP)-$Mg(NO_3)_2$ films (PA02, PA06, PA08, PA10, and PA14) are shown in Figure 1. The pattern of PA00 indicates the semicrystalline nature. The peaks present at $2\theta = 17.8°$, 19.3°, 21.2°, and 26.2° are due to the characteristic (100), (020), (110), and (021) planes of P(VDF-HFP), which are indexed with the standard XRD patterns of PVDF.[13] The peak at 21.2° corresponds to the β phase crystallization whereas, the other three peaks correspond to the α phase crystallization.[14]

Figure 1(b) is drawn for low values of 2θ ranging from 15 to 30° in order to analyze the possible changes in the peaks with the inclusion of $Mg(NO_3)_2$. It is observed from the patterns of PA02 to PA14 films that there is a broadening of (110) and (100) peaks, shift in (110) peak, and missing of (020) and (021) peaks. The peak shift of (110) indicates the interaction between the β phase polymer and the additive, whereas the broadening of (110) and (100) represents the reduced dimension of crystals. The missing of (020) and (021) peaks also indicates the reduction of the α phase. Hence, the changes in the patterns prove the reduction of the non-electroactive α phase in the polymer matrix, as well as the interaction of the β phase polymer with the additive of $Mg(NO_3)_2$. It is noticed that $Mg(NO_3)_2$ favors the polymer to crystallize in the electroactive β phase that induces its ferroelectric nature. This observation is similar to the report made by Dong *et al.* that the addition of 1-butyl-3-methylimidazolium [BMIM] bis(trifluoromethylsufonyl)imide [TFSI] into the polymer containing cations and anions could promote the β phase due to the presence of ions and their polarity.[15] The average crystallite size of $D_{(110)}$ is calculated using Debye Scherrer equation[13] and is found to be 16 nm.

FTIR spectra of P(VDF-HFP) film and P(VDF-HFP)-$Mg(NO_3)_2$ films are shown in Figure 2. The absorption spectra lying within

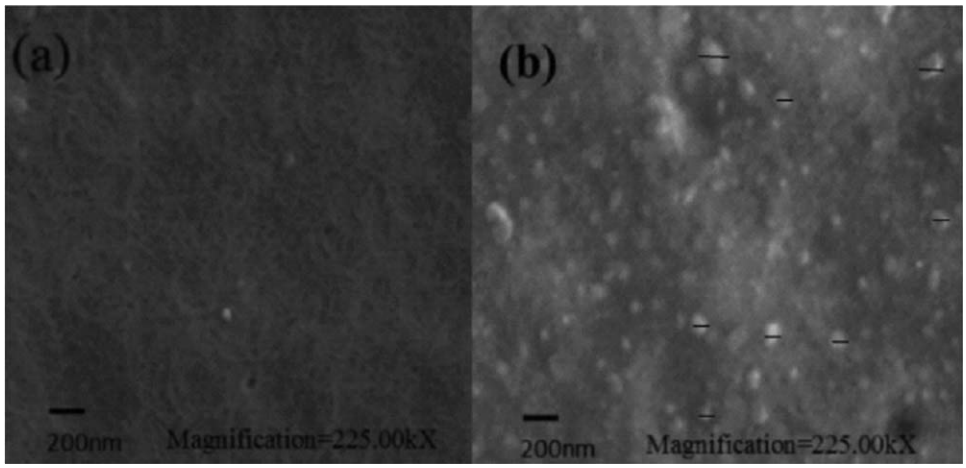

Figure 3. SEM images of (a) P(VDF-HFP) film and (b) P(VDF-HFP)-$Mg(NO_3)_2$ PA06 film.

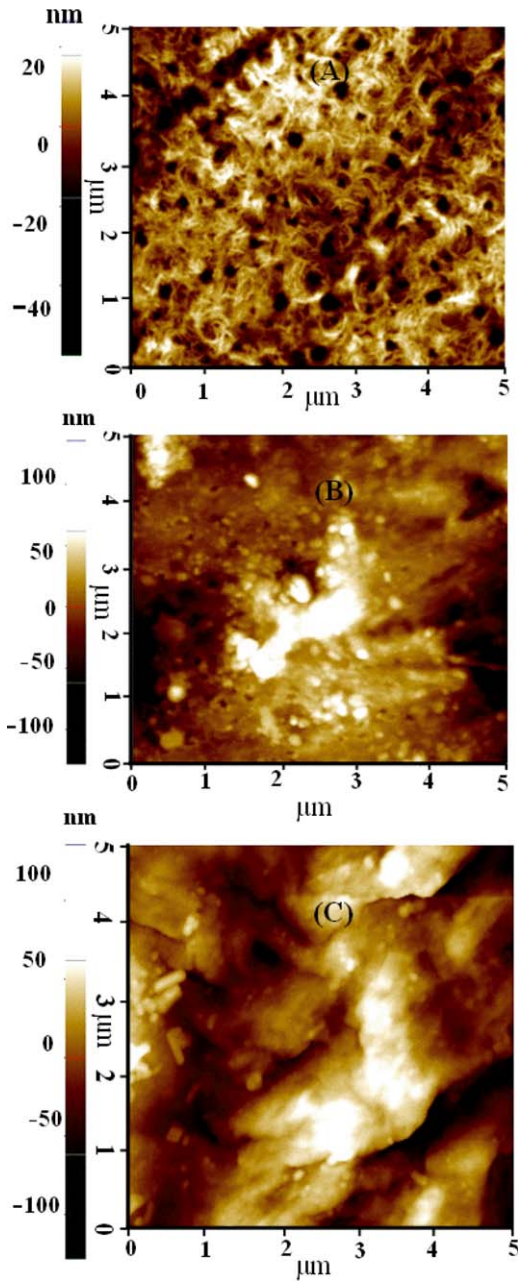

Figure 4. 2D AFM images of P(VDF-HFP) (a) PA00 film and P(VDF-HFP)-$Mg(NO_3)_2$, (b) PA08, and (c) PA10 films. [Color figure can be viewed in the online issue, which is available at wileyonlinelibrary.com.]

1,000–1,400 cm^{-1} correspond to the C—F stretching of the strong vibration band. The bands at 836 and 875 cm^{-1} are characteristic of all-trans sequences. Table I represents the characteristic vibrations assigned to the absorption bands. In sample PA00 the absorption bands observed at 612, 757, 794, 855, 875, 977, 1,165, and 1,179 cm^{-1} are assigned to the non-polar α phase and the peaks present at 836, 1,070, and 1,227 cm^{-1} are assigned to the β phase.[16–19] Further, it can be observed from the spectra that after the incorporation of magnesium nitrate into the P(VDF-HFP) matrix, the absorption bands corresponding to the α phase partially disappear, and on the other hand, the polar β phase is found to emerge. Although there is no

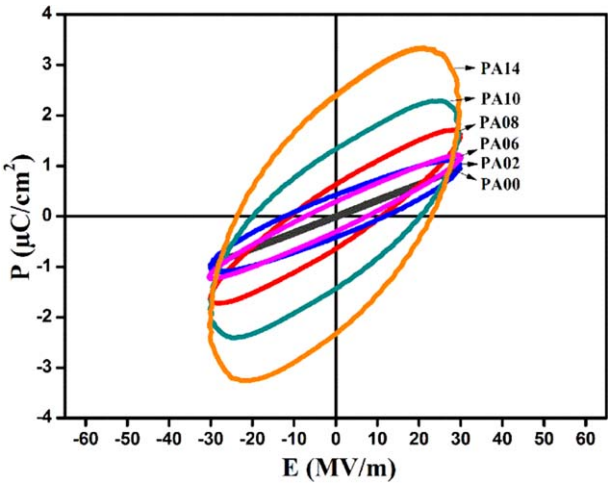

Figure 5. Ferroelectric hysteresis loops of P(VDF-HFP) film and P(VDF-HFP)-$Mg(NO_3)_2$ films. [Color figure can be viewed in the online issue, which is available at wileyonlinelibrary.com.]

discernible change of peaks in the FTIR pattern observed upon increasing the composition of $Mg(NO_3)_2$, there is an increase of intensities with the increase of the additive concentration. This confirms the increase of the crystalline order in the matrix with the inclusion of $Mg(NO_3)_2$.[14] Thus, the FTIR spectra also confirm the enhancement in the electro-active β-phase in the polymer with $Mg(NO_3)_2$ content.

The SEM micrographs of PA00 and PA06 films with the magnification of 225 kX are shown in Figure 3. In Figure 3(a), the plain P(VDF-HFP) film shows a smooth and uniform surface with a fiber-like structure.[20,21] Figure 3(b) reveals that $Mg(NO_3)_2$ is dispersed into the polymer uniformly and forms the nodular morphology on the top. The average size of nodules is found to be 120 nm.

The 2D topography of the films is analyzed with AFM and is described in terms of the surface roughness. Small area scan (5 × 5 μm) images are obtained through the non-contact mode and are shown in Figure 4.

Like the SEM micrograph in Figure 3(a), the AFM image in Figure 4(a) also shows the common fiber-like morphology of P(VDF-HFP) which turns into a nodule-like morphology (refer Figure 4(b,c) with the inclusion of $Mg(NO_3)_2$. This can further be explained as the $Mg(NO_3)_2$ behaving like a nucleating agent that tends to reduce the surface energy, which leads to the

Table II. The Values of Maximum Polarization at 30 MV/m, Remanent Polarization, and Coercive Field

Sample code	Pmax (μC/cm²)	Pr (μC/cm²)	Ec (MV/m)
PA00	0.9	0.03	1.2
PA02	1.0	0.4	11.8
PA06	1.1	0.2	7.5
PA08	1.6	0.6	11.1
PA10	1.8	1.3	20.6
PA14	3.2	2.4	23.0

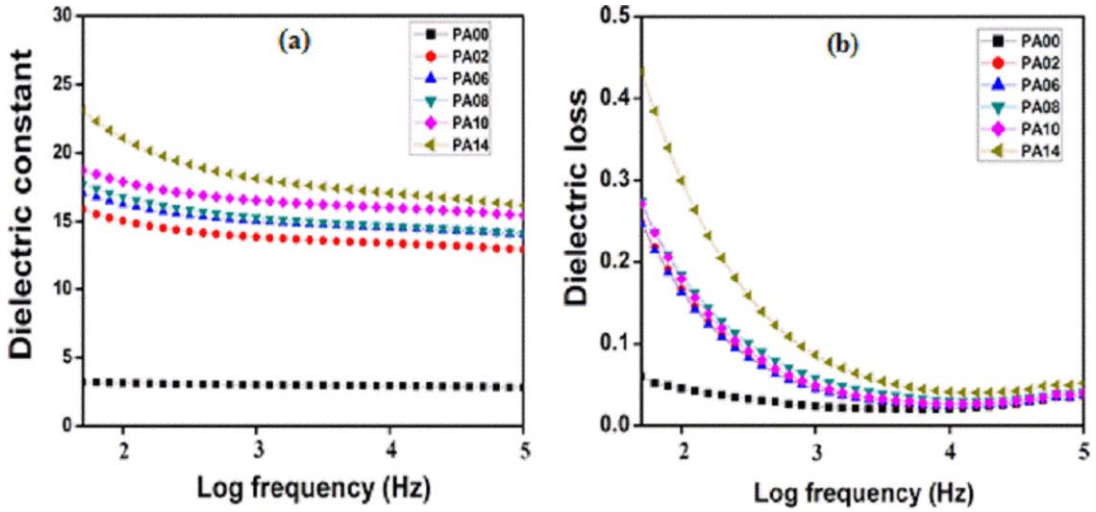

Figure 6. Plots of (a) Dielectric constant and (b) Dielectric loss as function of frequency. [Color figure can be viewed in the online issue, which is available at wileyonlinelibrary.com.]

formation of nodules.[22,23] The surface roughness is characterized by the average roughness parameter (Ra), and that of the plain polymer is found to be 6 nm. With the addition of $Mg(NO_3)_2$, the surface roughness values are found to increase systematically as 23 nm for PA08 and 35 nm for PA10. This indicates that the roughness of the surface is increased by the formation of nodules.

The ferroelectric properties of plain P(VDF-HFP) film and P(VDF-HFP)-$Mg(NO_3)_2$ films are studied by tracing the P–E loops at room temperature, these are presented in Figure 5. As seen from the Figure 5, the loops are symmetrical in the positive and negative applied potentials. PA00 exhibits a narrow symmetrical loop with low values of remnant polarization (Pr) and coercive field (Ec), which can be attributed to the predominance of a non-electro active α phase in the plain polymer film. As the $Mg(NO_3)_2$ content increases, the loops get wider and the Pmax, Pr, and Ec values are found to increase.

From Table II, it is observed that PA14, the sample having the highest $Mg(NO_3)_2$ content, exhibits the highest Pmax value of 3.2 μC/cm^2 at 30 MV/m. From the shape and size of the P–E loops, and also from the above results, it is understood that the incorporation of magnesium nitrate in the PVDF-HFP matrix induces an appreciable increase in the electroactive β phase crystallization. The addition of magnesium nitrate into the polymer increases the cations and anions, which could promote the β phase due to the presence of ions and their polarity. Also, $Mg(NO_3)_2$ behaves as the heterogeneous nucleation centers for ferroelectric domains during the polarization and hence, there is enhancement of the ferroelectric properties of the films, as evidenced by the XRD and FTIR studies. While applying the electric field, all the films have experienced an electrical breakdown at 30 MV/m.

The variation of dielectric constant with respect to the variation of frequency is shown in Figure 6(a) and the values obtained at 50 Hz are given in Table III. The dielectric constant varies from 3.2 to 23.2 at 50 Hz and from 2.8 to 16.7 at 100 kHz with the incorporation of magnesium nitrate. Moreover, in the PVDF based molecules, as the polarization is decided by the crystalline domains and β-phase,[24] the increase in the dielectric constant can be attributed to the changes in domains and the enhancement in the β phase created by the additive $Mg(NO_3)_2$ and also to the higher ionic conductivity offered by the dissociation of Mg^{2+} and NO_3^- ions. The frequency dependent dielectric loss is shown in Figure 6(b), which decreases gradually as similar to the dielectric constant, and reaches a value of 0.05 over the frequency range of 50 Hz to 100 kHz. Though the incorporation of magnesium nitrate leads to increase in the dielectric loss at low frequency, it maintains the value as low as possible at high frequency.

It is observed that the dielectric constant and dielectric loss values are large at low frequencies, and decrease gradually at higher frequencies. The high values at low frequencies can be attributed to the electrode polarization effect due to the accumulation of charge at the electrode–polymer composite interface and space charge effect, as reported by Ramesh *et al.*[25] At high frequencies, the dipoles are unable to follow the fast changing of alternative electric field hence, the polarization decreases, thereby decreasing the values of dielectric loss and dielectric constant.[25,26]

As leakage current is the major drawback observed in ferroelectric materials, the films are also subjected to leakage current

Table III. The Values of Dielectric Constant and Loss at 50 Hz

Concentration of $Mg(NO_3)_2$ (wt %)	Dielectric constant	Dielectric loss
0	3.2	0.05
2	15.8	0.24
6	17.0	0.25
8	17.8	0.27
10	18.7	0.28
14	23.2	0.43

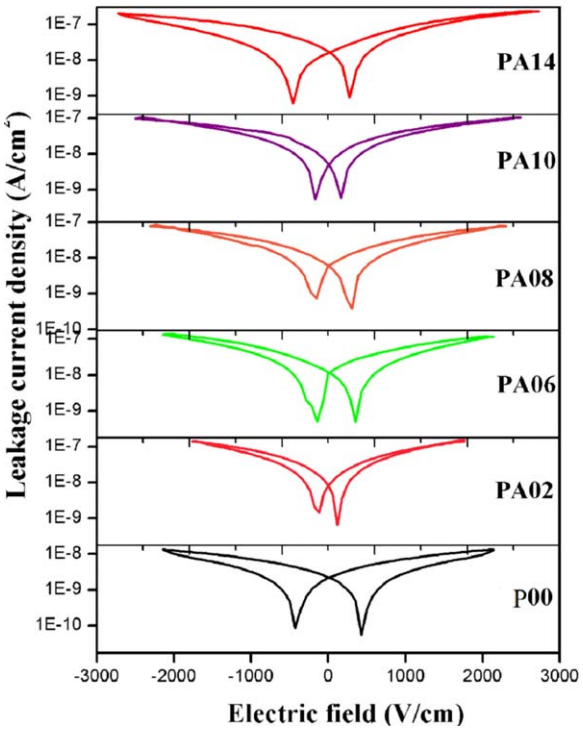

Figure 7. J–E loops of P(VDF-HFP) film and P(VDF-HFP)-$Mg(NO_3)_2$ films. [Color figure can be viewed in the online issue, which is available at wileyonlinelibrary.com.]

tests. The leakage current density (J) is obtained for various electric fields (E) and plotted as shown in Figure 7. The J–E loops of all the films show the non-linear behavior of the butterfly-like loop, which is the characteristic property of ferroelectric materials.

The leakage current density is in the order of 10^{-11} to 10^{-8} A/cm^2 for the plain film (PA00) in the range of −2,000 to 2,000 V/cm. However, for the films with $Mg(NO_3)_2$, it is in the order of 10^{-10} to 10^{-7} A/cm^2. Figure 7 shows that the increase of additive increases the leakage current density by 10 times. The common dielectric leakage mechanisms in polymer films are the Poole-Frenkel and Schottky effects shown in Figure 8.[27] The Poole-Frenkel effect[28] arises due to the field-assisted emission of electrons from the columbic traps in dielectrics and is given by

$$J = CE\ \exp\left\{-\frac{q\Phi-\beta\sqrt{E}}{\xi KT}\right\} \quad (1)$$

where C is the proportionality constant and ξ is called the slope parameter of the Poole-Frenkel effect. The Schottky effect[29] is the electric field-induced lowering of the barrier, which naturally forms at the interface between a metal and an insulator and strongly influences the leakage current in polymer films. It is represented by the Richardson-Dushman equation,

$$J = AT2\ \exp\left\{-\frac{q\Phi-\frac{1}{2}\beta\sqrt{E}}{KT}\right\} \quad (2)$$

where A is the Richardson constant, T is the absolute temperature, Φ is the barrier height, K is the Boltzmann's constant, and β is a material constant. The plot of ln (J/E) versus √E shown in Figure 8(a) does not linearly fit with the applied electric field, proving the absence of the Poole-Frenkel conduction mechanism.

The plot of ln (J) versus √E shown in Figure 8(b) is yields characteristic linear lines with $R^2 = 0.9$, which proves the presence of the Schottky effect in the films.

The sample area of 5 × 5 μm^2 is scanned by applying the tip bias of +10 V and −10 V alternately. The ferroelectric domains in the films tend to align in the direction of the applied bias. Hence, in Figure 9(a,b) the areas subjected to +10 V of bias are seen brightly, as the polarization aligns upwards, and the alternate areas subjected to −10 V of bias appear dark, as the polarization aligns downwards.

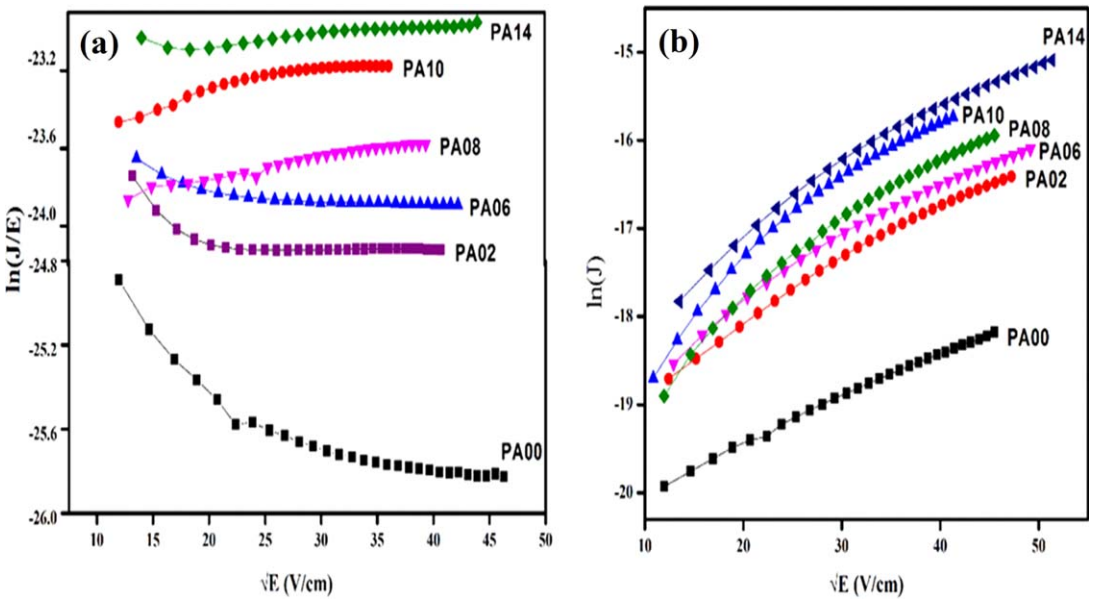

Figure 8. (a) Poole-Frenkel effect and (b) Schottky effect of films P(VDF-HFP) film and P(VDF-HFP)-$Mg(NO_3)_2$ films. [Color figure can be viewed in the online issue, which is available at wileyonlinelibrary.com.]

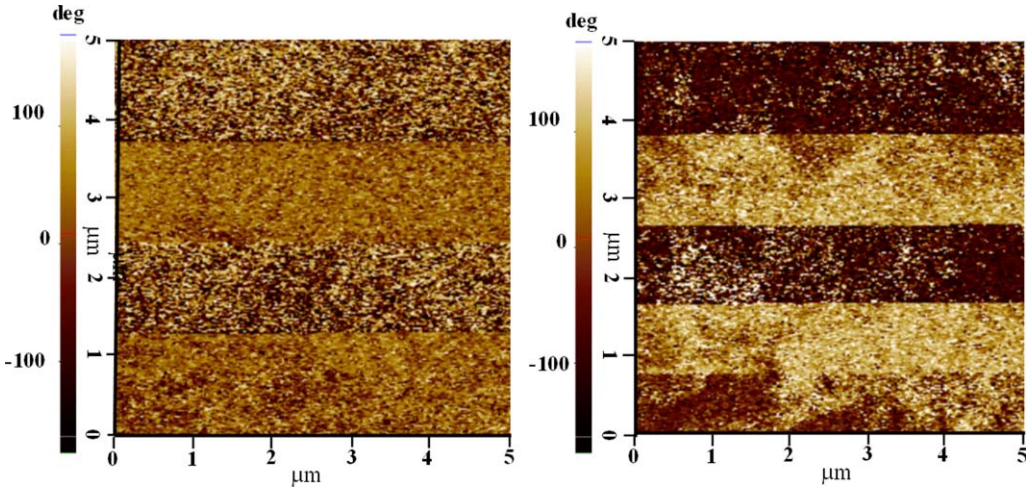

Figure 9. 2D-PFM phase images of sample (a) P(VDF-HFP) film (b) P(VDF-HFP)-$Mg(NO_3)_2$ PA14 film. [Color figure can be viewed in the online issue, which is available at wileyonlinelibrary.com.]

The areas in Figure 9(b) appear brighter and darker than those observed in Figure 9(a), which shows the influence of magnesium nitrate in P(VDF-HFP) on the switching of the ferroelectric domains.[30]

CONCLUSIONS

This article provides a systematic investigation on the enhancement of the electroactive β phase, in free-standing, flexible P(VDF-HFP) films induced by the incorporation of magnesium nitrate. The structural and compositional studies made by XRD and FTIR spectroscopy confirm the enhancement of the electroactive β phase in the films. The fibrous structure of the polymer changes to a nodule-like morphology with increasing roughness, as a result of the increasing magnesium nitrate content. The maximum polarization observed is 3.2 $\mu C/cm^2$ for the film with 1.4 wt % of magnesium nitrate salt, when it is subjected to the electric field of 30 MV/m. The dielectric constant and dielectric loss of the films follow a similar trend of being high at low frequencies and low at high frequencies. Higher leakage current density is observed in the P(VDF-HFP)-$Mg(NO_3)_2$ films than that of plain P(VDF-HFP) films, by an order of 10. The root cause for this increase in leakage current is proved to be the Schottky effect, that lowers the barrier at the polymer-$Mg(NO_3)_2$ interfaces. The piezo response of P(VDF-HFP)-$Mg(NO_3)_2$ confirms the ferroelectric switching behaviors. In addition to the enhanced and functional ferroelectricity, the piezoelectric properties, the cost effective fabrication method, flexible structure, and porous-free nature, suggest that these films would be suitable for device applications in energy storage, ferroelectric memory, actuators, and sensors.

ACKNOWLEDGMENTS

Authors would like to thank Department of Science and Technology (DST), Government of India for the financial support under the SERB project sanctioned to Dr. J. Hemalatha, Department of Physics, NIT, Tiruchirappalli. In addition, the authors acknowledge the Ministry of Human Resource and Development (MHRD), Government of India for the AFM facility under the plan fund sanctioned to the Department of Physics, NIT, Tiruchirappalli.

REFERENCES

1. Yang, L.; Li, X.; Allahyarov, E.; Taylor, P. L.; Zhang, Q. M.; Zhu, L. *Polym.* **2013**, *54*, 1709.
2. Guan, F.; Yang, L.; Wang, J.; Guan, B.; Han, K.; Wang, Q.; Zhu, L. *Adv. Funct. Mater.* **2011**, *21*, 3176.
3. Diasa, C. J.; Das-Gupta, D. K. *Appl. Phys.* **1993**, *74*, 6317.
4. Furukawa, T. *Phase Transitions* **1989**, *18*, 143.
5. Guan, F.; Wang, J.; Pan, J.; Wang, Q.; Zhu, L. *Macromolecules* **2010**, *43*, 6739.
6. Martins, P.; Lopes, A. C.; Lanceros-Mendez, S. *Prog. Polym. Sci.* **2014**, *39*, 683.
7. Nalwa, H. S. Ferroelectric Polymers Chemistry, Physics, and Applications, Marcel Dekker: New York, **1995**.
8. Ling, Q. D.; Liaw, D. J.; Zhu, C.; Chan, D. S. H.; Kang, E. T.; Neoh, K. G. *Prog. Polym. Sci.* **2008**, *33*, 917.
9. He, X.; Yao, K.; Gan, B. K. *Actuators, A* **2007**, *139*, 158.
10. Jayasuriya, A. C.; Schirokauer, A.; Scheinbeim, J. I. *J. Appl. Polym. Sci.* **2001**, *39*, 2793.
11. Tomer, V.; Manias, E.; Randall, C. A. *J. Appl. Phys.* **2011**, *110*, 044107.
12. Wegener, M.; Arlt, K. *Z. J. Phys. D: Appl. Phys.* **2008**, *4*, 165409.
13. Prabhakaran, T.; Hemalatha, J. *Mater. Chem. Phys.* **2013**, *137*, 781.
14. Ong, W.; Ke, C.; Lim, P.; Kumar, A.; Zeng, K.; Ho, G. W. *Polymer* **2013**, *54*, 5330.
15. Dong, Z.; Zhang, Q.; Yu, C.; Peng, J.; Ma, J.; Ju, X.; Zhai, M. *Ionics* **2013**, *19*, 1587.
16. Sousa, R. E.; Nunes-Pereira, J.; Ferreira, J. C. C.; Costa, C. M.; Machado, A. V.; Silva, M. M.; Lanceros-Mendez, S. *Polym. Test.* **2014**, *40*, 245.
17. Mandal, D.; Henkel, K.; Schmeiber, D. Control of the Crystalline Polymorph, Molecular Dipole and Chain Orientations in P(VDF-HFP) for High Electrical Energy Storage

Application, In Proceedings of the IEEE International Conference on Nanoscience, Technology and Societal Implications, Bhuvaneswar, India, December 8–10, **2011**, 1–5, IEEE. DOI: 10.1109/nstsi.2011.6111801.

18. Ostasevicius, V.; Milasauskaite, I.; Dauksevicius, R.; Baltrusaitis, V.; Grigaliunas, V.; Prosycevas, I. *Mechanika* **2010**, *86*, 78.
19. Prabhakaran, T.; Hemalatha, J. *Sci. Adv. Mater.* **2014**, *6*, 9.
20. Stephan, A. M. *Eur. Polym. J.* **2006**, *42*, 21.
21. Stephan, A. M.; Saito, Y. *Solid State Ionics* **2002**, *148*, 475.
22. Cardea, S.; Gugliuzza, A.; Sessa, M.; Aceto, M. C.; Drioli, E.; Reverchon, E. *ACS Appl. Mater. Interfaces* **2009**, *1*, 1171.
23. García-Payo, M. C.; Essalhi, M.; Khayet, M. *J. Membr. Sci.* **2010**, *347*, 209.
24. Tong, W.; Zhang, Y.; Yu, L.; Luan, X.; An, Q.; Zhang, Q.; Lv, F.; Chu, P. K.; Shen, B.; Zhang, Z. *J. Phys. Chem. C* **2014**, *118*, 10567.
25. Ramesh, S.; Ling, O. P. *Polym. Chem.* **2010**, *1*, 702.
26. Prabakaran, K.; Mohanty, S. M.; Nayak, S. K. *J. Mater. Sci. Mater. Electron.* **2014**, *25*, 4590.
27. Park, S. H.; Lee, D. C. *J. Korean Chem. Soc.* **1999**, *35*, 431.
28. H. Bottger, V.V. Bryksin. Hopping Conduction in Solids, Springer: Berlin, **1991**.
29. Mott, N. F.; Davis, E. A. Conduction in Nanocrystalline Materials; Clarendon Press: Oxford, **1979**.
30. Baji, A.; Mai, Y. W.; Li, Q.; Liu, Y. *Compos. Sci. Technol.* **2011**, *71*, 1435.